System identification of a mechanical system with impacts using model reference adaptive control

D. W. Virden* and D. J. Wagg

Automatic Control Laboratory, Department of Mechanical Engineering, University of Bristol, Queens Building, Bristol BS8 1TR, UK.

Abstract

A single degree of freedom mechanical spring-mass system was considered where the motion of the mass is constrained by an adjustable rigid impact stop. A model reference adaptive control algorithm combined with interspike interval techniques was used to consider the viability of identifying system parameters when impacts are present. The unmodified adaptive control algorithm destabilizes during vibro-impact motion, so three modified control algorithms were tested experimentally. The first, the *gain reset*, was found to be of limited use and system identification cannot be successfully carried out. The second and third used a *gain pause* strategy. The second algorithm used *acceleration triggering* and represented an improvement on the *gain reset* method. The third approach used *displacement triggering* and was found to be partially successful in identifying system parameters in the presence of vibro-impact motion.

Keywords: Adaptive control, system identification, vibro-impact, interspike intervals.

---

*Author for correspondence: dave.virden@bristol.ac.uk

Notation:

a_{ij}	Element of plant matrix
$\mathbf{A}$	Plant matrix
$\mathbf{A_m}$	Model plant matrix
$\mathbf{A_{md}}$	Discrete model plant matrix
b_i	Element of controller matrix
$\mathbf{B}$	Controller matrix
$\mathbf{B_m}$	Model controller matrix
$\mathbf{B_{md}}$	Discrete controller plant matrix
$b(t)$	Spike train time series
c	Damping constant
H	Spike train threshold
k	Spring constant
k_m	Controller constant
$\mathbf{K}$	Adaptive feedback gain
$\mathbf{K_r}$	Adaptive feedforward gain
m	Mass constant
$\boldsymbol{r}$	Reference signal
S	Samples recorded during impact
t_s	Model settling time
$\boldsymbol{u}$	Control output
$\boldsymbol{x}$	Displacement of mass
$\dot{\boldsymbol{x}}$	Velocity of mass
$\boldsymbol{x_m}$	Reference model displacement
$\dot{\boldsymbol{x}}_{\boldsymbol{m}}$	Reference model velocity
$\boldsymbol{x_e}$	System error
$\dot{\boldsymbol{x}}_{\boldsymbol{e}}$	Derivative of system error
α	MCS gain parameter
β	MCS gain parameter
Δ	Discrete sampling rate (samples/second)
τ_c	Time of contact (impact)
ζ	Damping ratio

1 INTRODUCTION

Systems with motion limiting constraints occur in many areas of mechanical engineering. For example, machines (Perterka & Kotera 1995), geared systems (Theodossiades & Natsiavas 2001, Karagiannis & Pfeiffer 1991), bearings (Neilson & Gonsalves 1993) and railway wheels (Knudsen *et al.* 1992). These types of systems present particular challenges in terms of mathematical modeling and control due to the nonlinear effects caused by impacts which occur during dynamic excitation.

Of the control techniques available, adaptive control allows a great deal of flexibility when dealing with uncertain or time varying plant parameters, and for this work a model reference type adaptive controller was used with no prior tuning (Stoten 1993). The mechanisms for destabilization of MRAC controllers are well known; (Ioannou & Kokotovic 1984, Anderson *et al.* 1986), but systems with constraints present a particular challenge to developing a stable and robust adaptive control strategy (Zavala-Rio & Brogliato 2001, Tung, Wang & Hong 2000).

(McCarragher & Austin 1998, Zavala-Rio & Brogliato 2001, and Tung *et al.* 2000) study the problem of using adaptive control techniques to control robot manipulators with constraints (i.e. impacts). Related work by (Kárason & Annaswamy 1994) and (Annaswamy & Wong 1997) examines the behavior of adaptive control in the presence of input constraints and saturation. In this paper the viability of using a model reference adaptive control algorithm to identify system parameters when motion limiting constraints produce impacts in the system is examined. The theoretical formulation of the control algorithm is outlined in section 2. In section 3 the experiential setup used for the control tests is described. The experimental results are discussed in section 4 and the performance of each algorithm during testing is described.

2 THEORETICAL FORMULATION

2.1 Control algorithm

In this work we use a model reference adaptive controller, known as the minimal control synthesis (MCS) algorithm (Stoten 1993). MCS is a form of model reference adaptive control that assumes no prior knowledge of the system parameters, and in which the adaptive control gains are all initially set to zero. We begin by considering the general linear state space formulation for MCS. The plant state equation can be written in the form

$$\dot{\boldsymbol{x}}(t) = \mathbf{A}\boldsymbol{x}(t) + \mathbf{B}\boldsymbol{u}(t) \tag{1}$$

where $\boldsymbol{x}$ is the state variable vector of dimension $n \times 1$, $\boldsymbol{u}$ the control signal, dimension $p \times 1$, $\mathbf{A}$ and $\mathbf{B}$ represent the linear dynamics of the plant.

The controller for the MCS algorithm is defined as

$$\boldsymbol{u}(t) = \mathbf{K(t)}\boldsymbol{x}(t) + \mathbf{K_r(t)}\boldsymbol{r}(t), \tag{2}$$

where $\boldsymbol{r(t)}$ is the reference (demand) signal, $\mathbf{K(t)}$ is the feedback adaptive gain and $\mathbf{K_r(t)}$ the feed forward adaptive gain. Substituting equation 2 into equation 1 gives

$$\dot{\boldsymbol{x}} = \mathbf{A}\boldsymbol{x} + \mathbf{B}(\mathbf{K}\boldsymbol{x} + \mathbf{K_r}\boldsymbol{r}) = (\mathbf{A} + \mathbf{BK})\boldsymbol{x} + \mathbf{BK_r}\boldsymbol{r}. \tag{3}$$

This type of controller operates without explicit values for the matrices $\mathbf{A}$ and $\mathbf{B}$. Instead, the plant is controlled to follow the output of a reference model with known dynamics of the form

$$\dot{\boldsymbol{x}}_{\boldsymbol{m}}(t) = \mathbf{A_m}\boldsymbol{x_m}(t) + \mathbf{B_m}\boldsymbol{r}(t), \tag{4}$$

where $\boldsymbol{x_m}$ is the state of the reference model and $\mathbf{A_m}$ and $\mathbf{B_m}$ are linear reference equivalents of $\mathbf{A}$ and $\mathbf{B}$. For the experiments a discrete time approximation, $\boldsymbol{x_{md}}$ was used as shown in Equation 5 using the parameters $\mathbf{A_{md}}$ and $\mathbf{B_{md}}$ from Equation 6

$$\boldsymbol{x_{md}}(t) = \mathbf{A_{md}}\boldsymbol{x_{md}}(t-1) + \mathbf{B_{md}}\boldsymbol{r}(t-1), \tag{5}$$

$$\mathbf{A_{md}} = \begin{bmatrix} 1 & \Delta \\ -16\Delta/t_s^2 & 1 - 8\Delta/t_s^2 \end{bmatrix}, \mathbf{B_{md}} = \begin{bmatrix} 0 \\ 16\Delta/t_s^2 \end{bmatrix} \qquad (6)$$

The performance of the controller is monitored using the error signal $\boldsymbol{x_e} = \boldsymbol{x_m} - \boldsymbol{x}$. The objective of the control algorithm is for $\boldsymbol{x_e} \to 0$ as $t \to \infty$. We can reformulate the dynamics of the system as the error dynamics using $\dot{\boldsymbol{x}}_e = \dot{\boldsymbol{x}}_m - \dot{\boldsymbol{x}}$ such that

$$\dot{\boldsymbol{x}}_e = \mathbf{A_m}\boldsymbol{x_e} + (\mathbf{A_m} - \mathbf{A} - \mathbf{BK})\boldsymbol{x} + (\mathbf{B_m} - \mathbf{BK_r})\boldsymbol{r}. \qquad (7)$$

Then providing $(\mathbf{A_m} - \mathbf{A} - \mathbf{BK}) \to 0$ and $(\mathbf{B_m} - \mathbf{BK_r}) \to 0$ the stability of the system will depend only on the matrix $\mathbf{A_m}$, which we can select in advance.

In general, the MCS gains are defined as

$$\begin{aligned} \mathbf{K} &= \alpha \int_0^t \boldsymbol{y_e}\boldsymbol{x(t)}\mathrm{d}t + \beta\boldsymbol{y_e}\boldsymbol{x(t)} \\ \mathbf{K_r} &= \alpha \int_0^t \boldsymbol{y_e}\boldsymbol{r(t)}\mathrm{d}t + \beta\mathbf{y_e}\mathbf{r(t)} \end{aligned} \qquad (8)$$

where $\boldsymbol{y_e} = \mathbf{C}\boldsymbol{x_e}$, and $\mathbf{C}$ is chosen such that the transfer function $\mathbf{C}(s\mathbf{I} - \mathbf{A})^{-1}\mathbf{B}$ is strictly positive real (SPR) (Hodgson & Stoten 1996). The control weightings α and β can be chosen to give the appropriate amount of adaptive effort. From empirical results we always maintain the ratio $\alpha/\beta = 10$ and $C = 4/t_s$ (Stoten 1993) (assuming first order control) where t_s is the required settling time of the plant. The MCS algorithm has been shown to be stable and robust for a wide range of $\mathbf{A}$ and $\mathbf{B}$ values (Hodgson & Stoten 1996; Hodgson & Stoten 1999; Stoten & Benchoubane 1990). Further details of implementing MCS for both first and second order systems can be found in (Stoten 1993).

2.2 System identification algorithm MCSID

The MCS control algorithm has been extended to a system identification algorithm by Stoten & Benchoubane (1993). The basic premise can be seen by comparing equations 4 and 3, from which we can see that for exact matching between the plant and the reference model, the following relations hold

$$\begin{aligned} \mathbf{A} + \mathbf{BK} &= \mathbf{A_m} \\ \mathbf{BK_r} &= \mathbf{B_m} \end{aligned}. \qquad (9)$$

Therefore it should be possible identify the unknown parameter matrices $\mathbf{A}$ and $\mathbf{B}$ by computing

$$\mathbf{B} = \mathbf{B_m} \mathbf{K_r}^{-1}$$
$$\mathbf{A} = \mathbf{A_m} - \mathbf{B}\mathbf{K}$$
\qquad (10)

assuming that $\mathbf{K_r}^{-1}$ can be found (Stoten & Benchoubane 1993). The work carried out in Stoten & Benchoubane (1993) relies on the system matrices, $\mathbf{A}$ and $\mathbf{B}$ having the following specific phase-canconinal form,

$$\mathbf{A} = \begin{bmatrix} \mathbf{A_{11}} & \dots & \mathbf{A_{1p}} \\ \vdots & & \vdots \\ \mathbf{A_{p1}} & \dots & \mathbf{A_{pp}} \end{bmatrix}, \quad \mathbf{B} = \begin{bmatrix} \mathbf{B_{11}} & & 0 \\ & \ddots & \\ 0 & & \mathbf{B_{pp}} \end{bmatrix}, \qquad (11)$$

where

$$\mathbf{A_{ii}} = \begin{bmatrix} 0 & 1 & 0 & \dots & 0 \\ 0 & 0 & 1 & \dots & 0 \\ \vdots & \vdots & \vdots & \ddots & \vdots \\ 0 & 0 & 0 & \dots & 1 \\ -a_{ii1} & -a_{ii2} & -a_{ii3} & \dots & -a_{iin_i} \end{bmatrix}, \qquad (12)$$

and

$$\mathbf{A_{ij}} = \begin{bmatrix} 0 & \dots & \dots & 0 \\ \vdots & & & \vdots \\ 0 & \dots & \dots & 0 \\ -a_{ij1} & -a_{ij2} & \dots & -a_{ijn_j} \end{bmatrix}, \quad \mathbf{B_{ii}} = \begin{bmatrix} 0 \\ \vdots \\ 0 \\ b_{ii} \end{bmatrix}. \qquad (13)$$

Here, n_i is the state dimension of the ith degree of freedom, such that $\sum_{i=1}^{p} n_i = n$. The reference model system matrices will have correspondingly similar structure.

A schematic representation of the system is shown in Figure 1, from which we derive the equation of motion for the spring mass-damper system as

$$m\ddot{x} + c\dot{x} + kx = k_m u \qquad (14)$$

where x is the displacement of the mass and $\dot{x}$ is the velocity. In this model k_m is a constant which represents the combined motor, potentiometer and amplifier gains

for the single mass rig. Writing equation 14 in a first order form gives

$$\begin{bmatrix} \dot{x}_1 \\ \dot{x}_2 \end{bmatrix} = \begin{bmatrix} 0 & 1 \\ -k/m & -c/m \end{bmatrix} \begin{bmatrix} x_1 \\ x_2 \end{bmatrix} + \begin{bmatrix} 0 \\ k_m/m \end{bmatrix} u \tag{15}$$

Thus we have a (2×2) **A** matrix and a (2×1) **B** matrix with the values

$$\begin{aligned} a_{21} &= -k/m \\ a_{22} &= -c/m \\ b_{21} &= k_m/m \end{aligned} \tag{16}$$

and $a_{11} = 0, a_{12} = 1, b_{11} = 0$.

2.3   Interspike intervals

Interspike intervals can be used to identify or reconstruct dynamic characteristics of a system from examining the intervals between a series of spikes or pulses (Sauer 1994). For impacting systems this can be applied to intervals between successive impacts (Wagg *et al.* 1999). A key requirement for interspike interval techniques is the accurate measurement of the spikes. Impulse spikes which occur in impacting systems with hard materials (e.g. steel on steel) are usually very short time events. The time of contact, τ_c, is related by S and Δ such that $\tau_c \approx S/\Delta$, where Δ is the digital sampling rate, and S is the number of samples recorded during contact. In this work we use an accelerometer attached to the impact stop (second algorithm) or displacement data (third algorithm) to produce a *spike train* signal $b(t)$. Therefore we need a suitably fast sampling rate, Δ, to ensure that we capture spikes to a sufficient level of accuracy. However, spikes only occur for a very short time, at relatively large intervals, so a very fast Δ will result in large quantities of unwanted data being recorded. We must also choose a suitably defined *threshold* value, H, to distinguish between spikes and noise. Thus $b(t) > H$ is recorded as a spike, and $b(t) < H$ is disregarded. The choice of H is arbitrary, but must be made from inspection of a spike train signal. Failure to set an appropriate H value can lead to the following scenarios:

1. Threshold value too high; low velocity impacts will be missed.
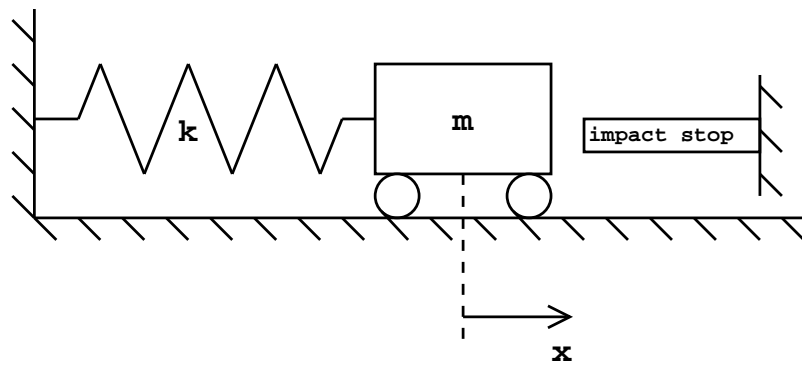
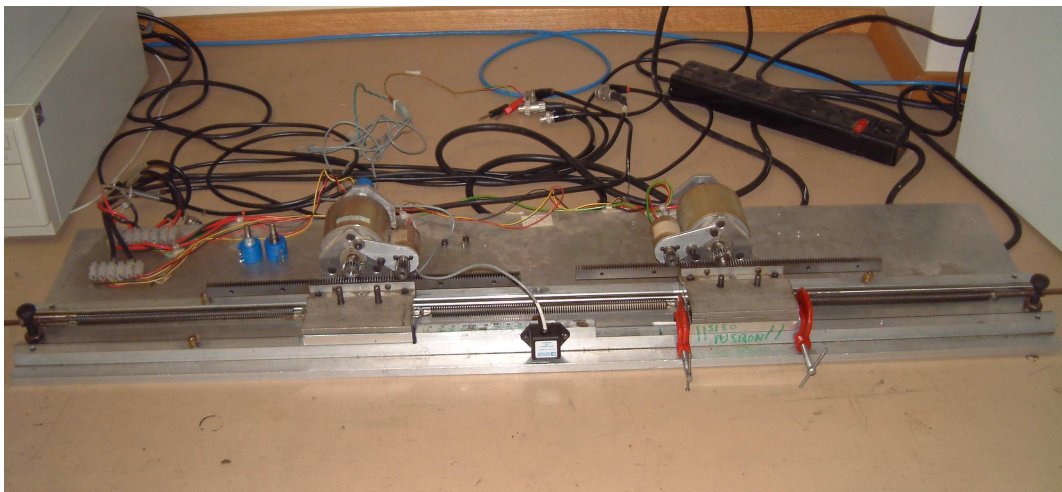Figure 1: Schematic of Rig

Figure 2: Photograph of Experimental Setup

2. Threshold value too low; noise peaks may be mistaken for impulse spikes.

These issues are discussed in detail in (Wagg *et al.* 1999)

3 EXPERMENTAL SETUP

A photograph of the experimental setup is shown in Figure 2. The mass is mounted on a uniaxial track with wheel bearings, and driven via a rack and pinion gearing. The second mass, which can be seen on the right hand side in the photo, was clamped rigidly for the duration of the tests. Springs between the two end stops and the masses themselves provide the restoring forces for the mass. In this

system damping occurs due mainly to the friction in the track and gear system. These components also introduce some nonlinearity due to friction in the bearings on which the mass oscillates.

The system had an adjustable mass which allowed the weight of the trolley to be changed. For these experiments two configurations were used which weighed 0.75kg and 1kg respectively. The damping and spring constants remained unchanged for the duration of the experiment.

The impact stop was constructed from a piece of square metal block that was clamped to the track bed $45mm$ from the centre of the motor. $3mm$ of high density foam was attached to the end of the block. From the impact spike data, impacts were observed to last for approximately 1/15 of a second.

The position of the mass was controlled via an electric motor, and the displacement and velocity of the mass was recorded using a potentiometer and tachometer respectively. The signals are read via an Amplicon PC30AT card, which is also used to output the control signal. The control system was implemented on a 486 Personal Computer running RedHat Linux 5.1. A sampling rate of 256Hz was used for all tests. This was controlled using the Linux real time clock.

Preliminary tests were carried out on the rig to identify the nature of the damping. This involved subjecting the rig to an impulse and observing the response. From these tests it was found that the system was close to critically damped, $\zeta \approx 1$.

For the work in this paper the MCS algorithm was implemented on the rig using the following parameters; $\alpha = 0.1$, $\beta = 0.01$ and $t_s = 1$ second. The reference signal was composed of three sine waves

$$r = 0.4\sin(2\pi t) + 0.133\sin(3\pi t) + 0.08\sin(5\pi t). \tag{17}$$

This reference signal was chosen to satisfy the persistence of excitation condition (Sastry & Bodson 1989; Stoten 1993). The discrete reference model (Equation 5) was used with the discrete reference model parameters (Equation 6) with $t_s = 1s$ and $\Delta = 1/256s$

For each test the MCS control was implemented with zero initial conditions and run for approximately 250 seconds when the adaptive control gains had stabilized.
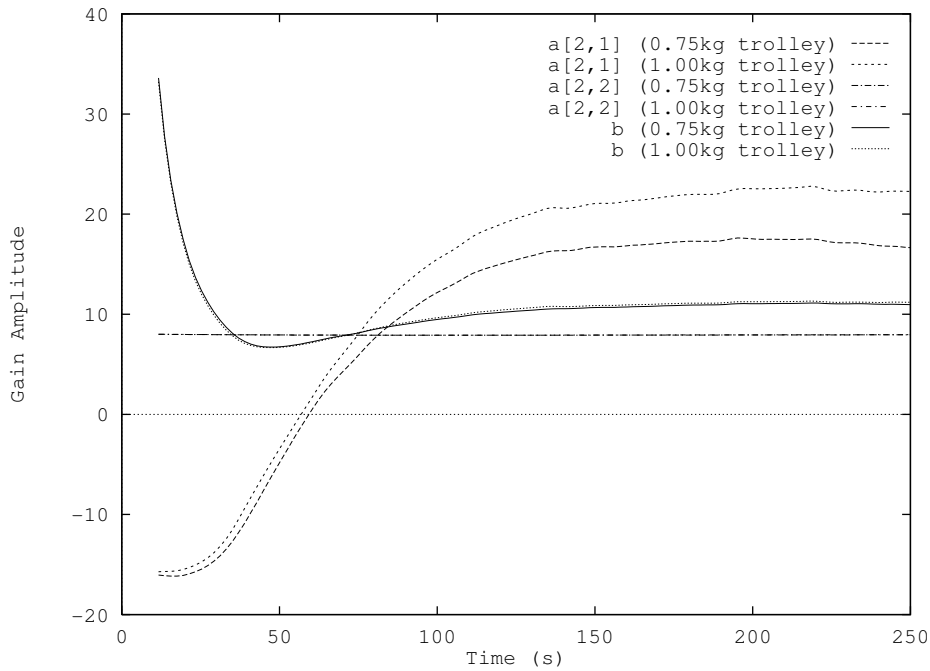
Figure 3: Non-impacting system parameters

The accelerometer was amplified using a customized DC amplifier and connected to an input channel on the Analogue to Digital Card (ADC). This signal was sampled at every control step and compared to the threshold to determine if an impact had occurred. The displacement spike train was computed from the displacement data and a predetermined threshold value H.

4 EXPERMENTAL RESULTS

4.1 Non-impacting system identifcation

The first set of tests were carried out to identify the parameters of the system with no impacts present. These values were then used to compare with the values found from the impacting tests. MCS system identification (MCSID) has already been carried out on this apparatus and reported in (Stoten & Benchoubane 1993), although this used different trolley mass values. Using the analysis developed in (Stoten & Benchoubane 1993) the parameters required to characterise the SISO
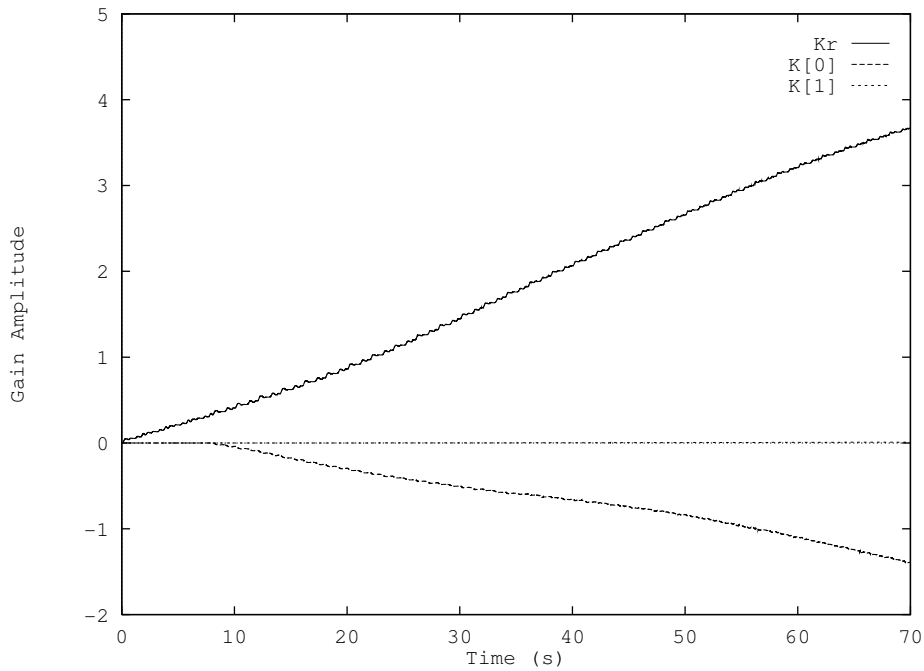
Figure 4: Gain Values from Unmodified Algorithm

system are

$$a_{21} = -k/m, \quad a_{22} = -c/m, \quad b_{21} = k_m/m \tag{18}$$

where k_m includes the potentiometer, motor and amplifier gains.

The results of the two tests are shown in Figure 3. Data was recorded from approximately 10 seconds after the test started. From Figure 3 we see that the parameter values have stabilized after a further 200 seconds. This experiment was run twice, once with each mass configuration. Dividing the settled value of the a_{21} parameter for each trolley configuration gave a ratio of 0.723 which is very favorable when compared to the predicted ratio of 0.75.

These results confirm the finding of (Stoten & Benchoubane 1993) that MCS can be used to identify the system parameters of electro-mechanical systems with governing equations that fit the specified phase-canonical form.
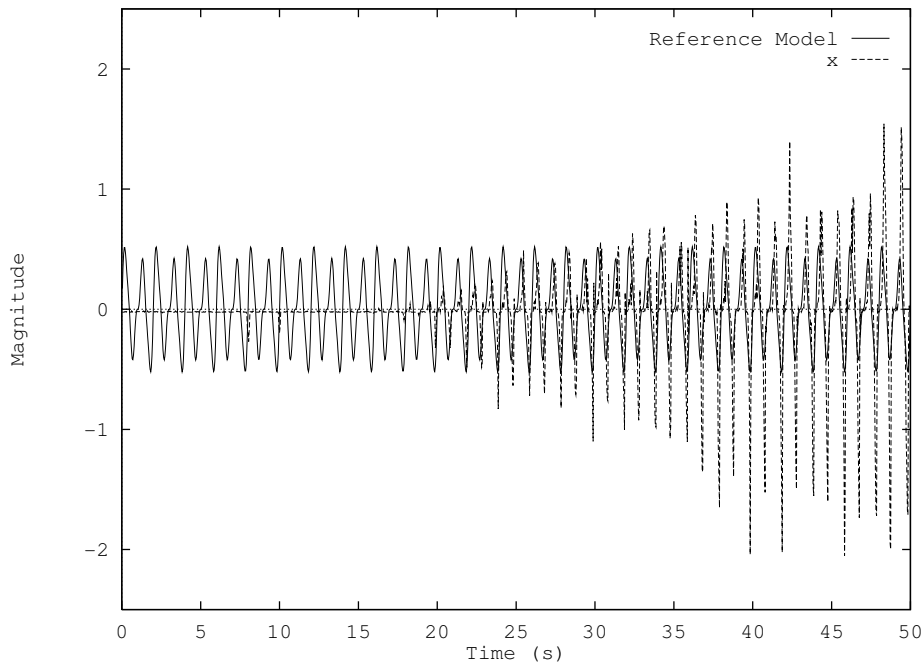
Figure 5: Displacement under Unmodified Algorithm

4.2   System identification with impacts

4.2.1   Unmodified algorithm

An initial test was carried out to see the effect of introducing an impact on the standard MCS control algorithm. For these tests $\mathbf{K_r} = k_r$ is scalar and $\mathbf{K} = [k[0], k[1]]^T$. The result of this test was that the control gains, k_r and $k[0]$ were found to increase steadily from time $t = 0$ in an approximately linear manner. This is shown in Figure 4, where we also note that gain $k[1]$ remains at an insignificantly small amplitude throughout the test. The increasing gain phenomena is known as "gain wind up", and will eventually lead to a sudden destabilization of the controller. In this example the mechanism behind the gain wind up is due to the introduction of a strong nonlinearity associated with the impact. In Figure 5 the displacement of the trolley under the unmodified algorithm is shown.

There are two components to the gain wind up shown in Figure 4. The first is the initial gain windup where the gains adapt to the steady state values observed in the non-impacting test (Figure 3). Once the gains have started to wind up the
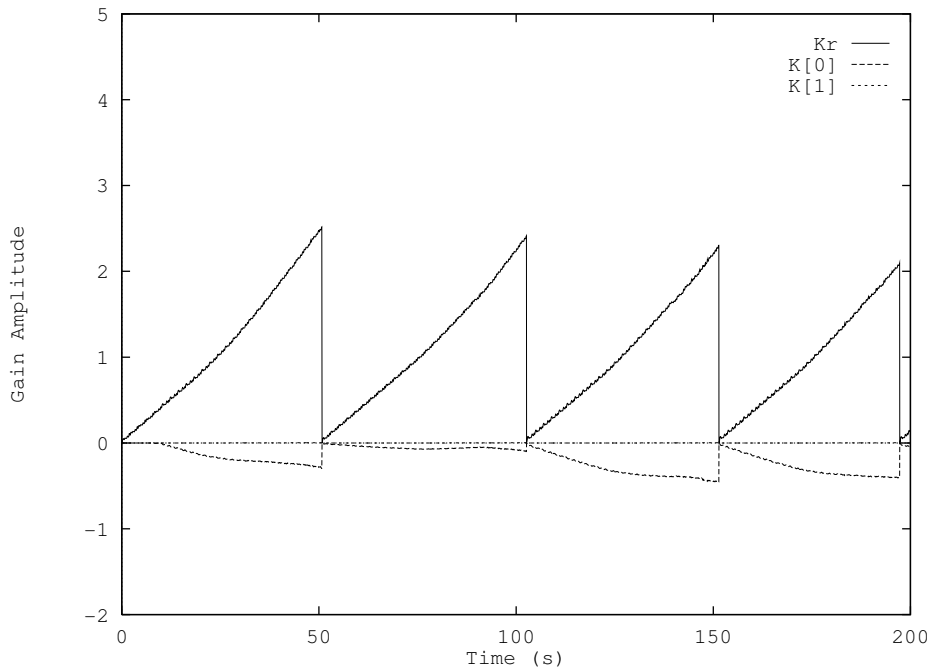
Figure 6: Gain Values from Gain Reset Algorithm

trolley moves and starts to impact. This can be seen in Figure 5 where the first impact occurs at approximately $27s$ with an amplitude of $\sim 0.45V$. This regular impact, with a period of $2s$, represents a strong non linearity which causes further controller gain windup which will eventually cause the unmodified algorithm to lose stability. The motion of the trolley gets less predictable as the gains continue to windup and its velocity increases. This results in the increased displacement seen after $37s$ in Figure 5. The spikes which are greater than $0.45V$ are due to the high impact velocities, which occur during the loss of stability, where at each impact a significant impulse force is transferred to the experimental apparatus.

4.2.2 Gain reset algorithm

The most simplistic approach to dealing with an impact (or other short time nonlinear event) during adaptive control is to simply reset the gains to zero. The MCS algorithm is based on starting all gains from zero, so in effect this is restarting the control algorithm again after each impact. The period of $50s$ between impacts is due to the controller having to readapt to its steady state values after being reset.
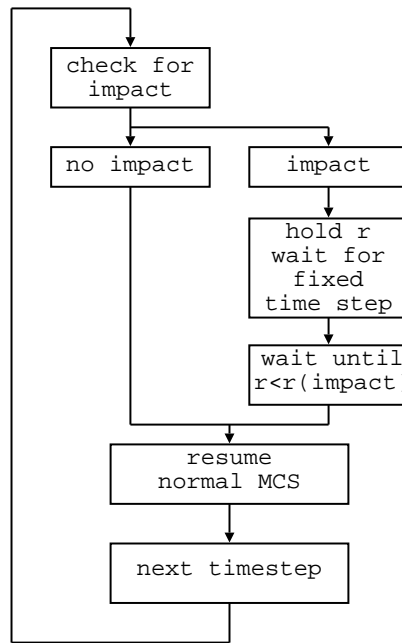
Figure 7: Schematic of Gain Pause Algorithm

For these tests an impact correlated to a spike of greater than the threshold value $H = 2.3$V from the accelerometer. The results from the test are shown in Figure 6, where we have plotted the control gains. Again we note that $k[1]$ is of such a small amplitude, that it is indistinguishable from the time axis. Although this approach proved successful in preventing gain wind up, it is very inefficient in terms of control, and could only be recommended if no other technique could be applied. It is certainly not suitable for application to a system with a periodic impact as the control suffers noticeably. However one potential application would be to implement the method as a safety mechanism, on systems where an impact is not normally expected. It is also clear from Figure 6 that system identification cannot be attempted using these results, as the gains do not have sufficient time between impacts to attain steady state values.

4.2.3   Gain pause algorithm

A second, more sophisticated strategy, is to pause the gain adaption during the time that the impact occurs. This algorithm was implemented by identifying a spike
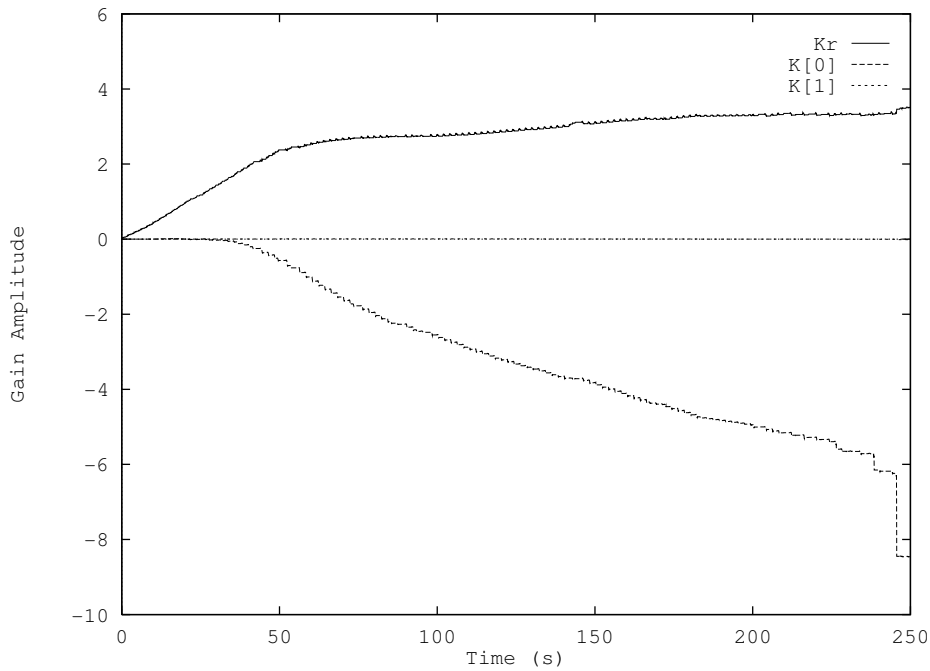
Figure 8: Gain Values from Gain Pause Algorithm (Acceleration Triggering)

as before, and then pausing adaption, initially for a fixed interval of 0.25 seconds, and waiting until the reference signal had dropped below the value that had caused the impact. The reference signal was not allowed to resume the original function until it was less than the value that caused the impact. The fixed interval of $0.25s$ was used in order to prevent the switch between adaption, pause and back to adaption occurring too rapidly — it was noted during tests that rapid switching could cause controller destabilisation as essentially this is a form of nonsmooth event itself. A schematic flow diagram showing the complete gain pause algorithm is shown in Figure 7.

The MCS gain values computed during a typical test are shown in Figure 8. We note that as with previous examples $k[1]$ is of negligible amplitude. From Figure 8 we can also see that although k_r reaches a steady state value, the absolute value of $k[0]$ increases steadily throughout the test, and has some step jumps in amplitude towards the final stages of the test. As a result, in this system, the system identification could only be carried out on the K_r gain data. The step increases in the $k[0]$ gain occurred due to a series of missed impacts.

In Figure 9, we have plotted the $(n-1)$th interval between spikes, ΔT_{n-1}, against
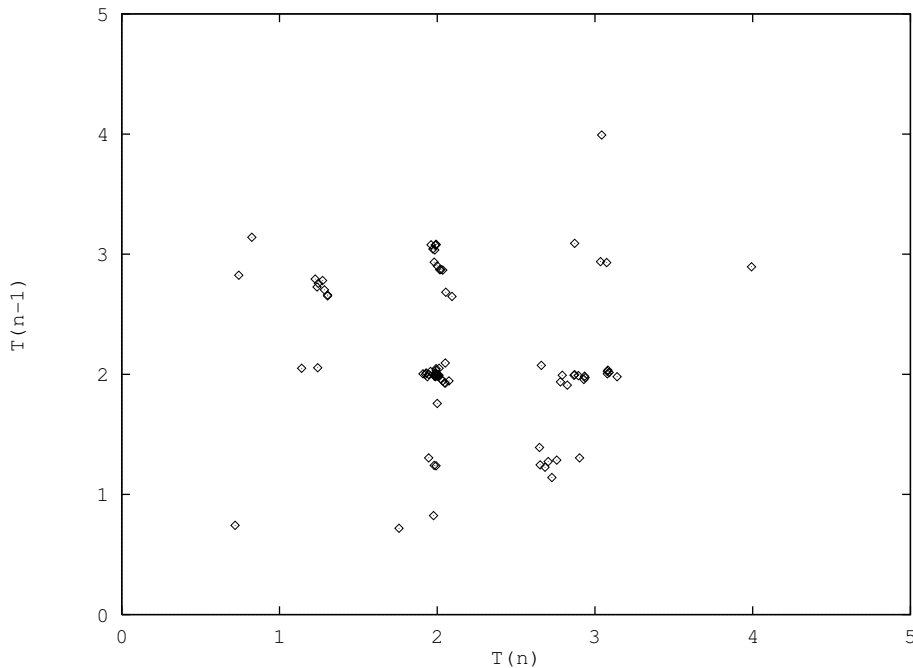
15

Figure 9: Interspike Intervals (Gain Pause, Acceleration Triggering)

the nth interval ΔT_n. For this test we see that the majority of impacts occurred at intervals of approximately 2 seconds. However, there are a range of other ΔT_n values, which mean that the interspike interval plot forms a grid like pattern. This grid layout is indicative of a general problem of missing spikes or identifying spurious spike — both cases are discussed in detail in (Wagg *et al.* 1999).

Figure 10 shows the threshold value, H, and the signal from the accelerometer used to calculate the interspike intervals.

4.2.4   Displacement triggering

The limitations of the preceding techniques in terms of system identification, led us to seek a more reliable approach. This was achieved by using the displacement of the trolley to determine when an impact had occurred, and to trigger the pause algorithm. It was found that using this technique the α and β adaptive gain parameters could be increased by a factor of 10 to $\alpha = 1$ and $\beta = 0.1$ This produced much more satisfactory system identification results as both gains leveled off quickly — although there were significant fluctuations in the stabilised gain values. This
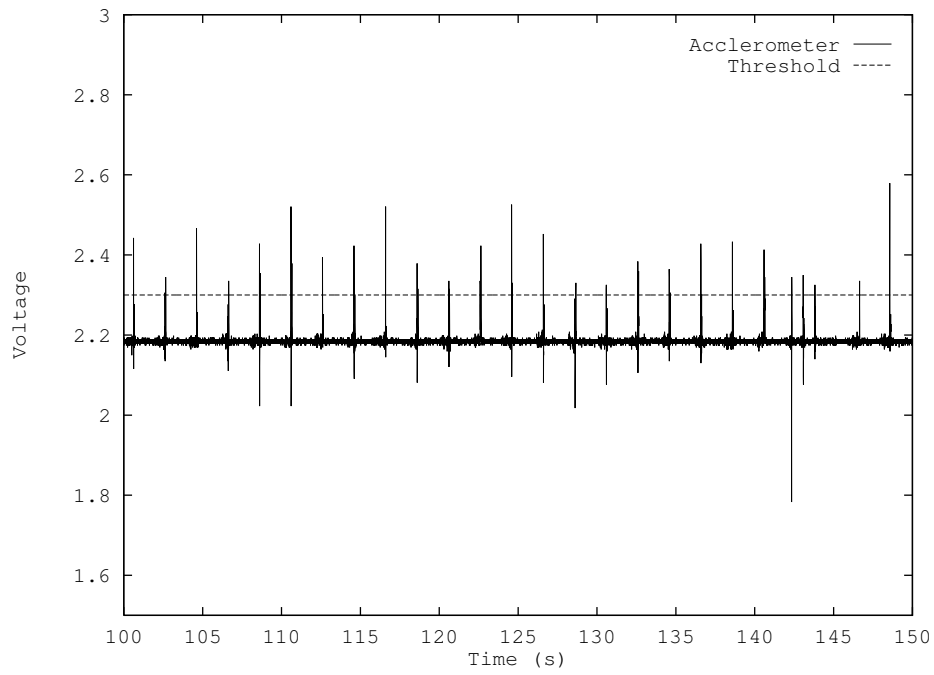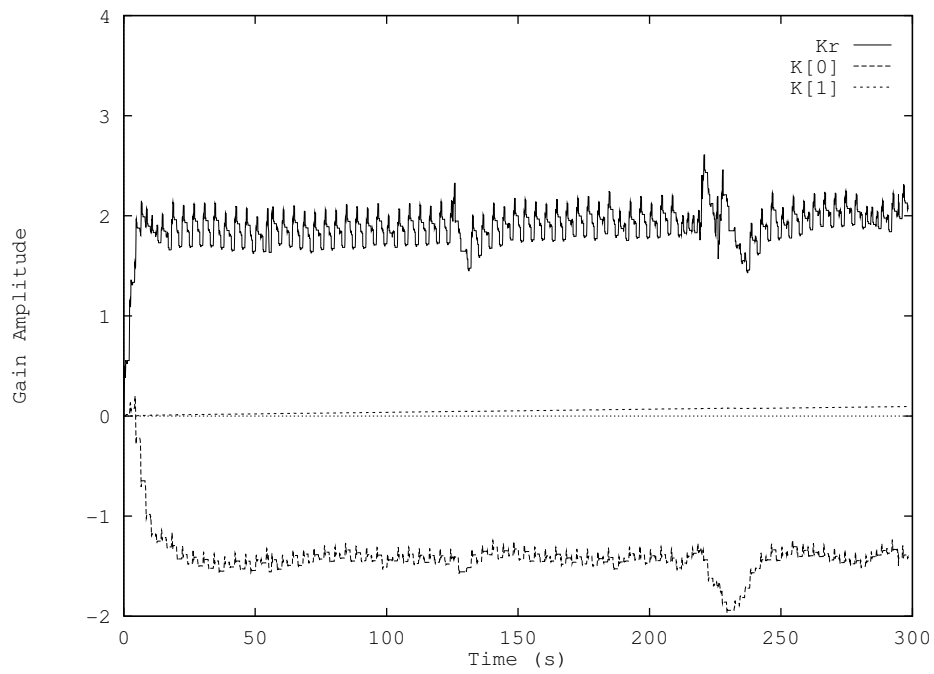
Figure 10: Spike Train and Threshold

Figure 11: Gain Values from Gain Pause Algorithm (Displacement Triggering)
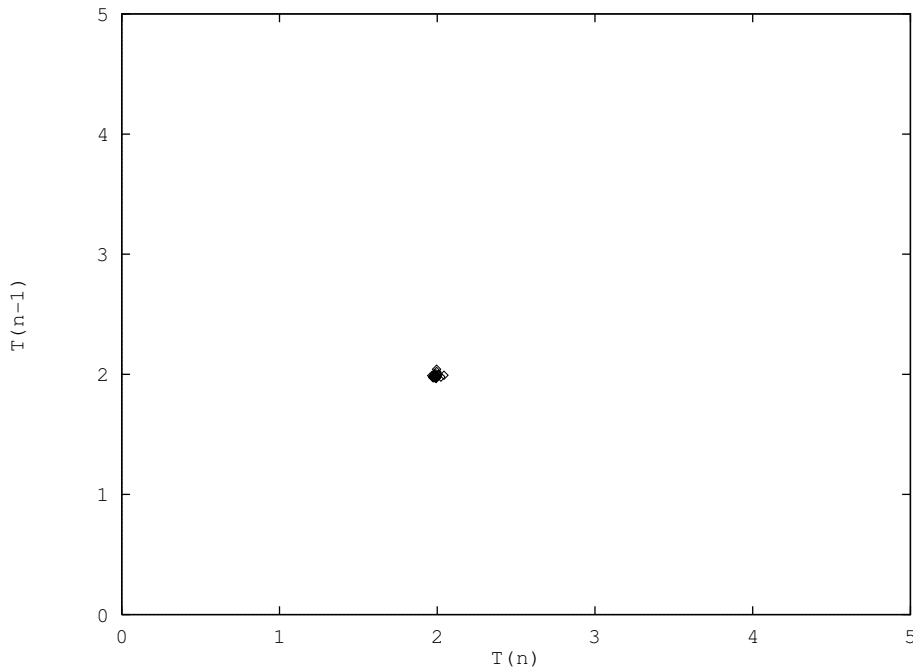
17

Figure 12: Interspike Intervals (Gain Pause, Displacement Triggering)

is shown in Figure 11, where we have plotted the MCS gain values for a typical displacement triggering test. The interspike interval plot for this test is shown in Figure 12. This shows that the motion is dominated by an interspike interval of $\Delta t \approx 2$. This indicates a predominately period one vibro-impact motion (Bishop *et al.* 1998), and shows that the problems with missed/spurious spikes have been eliminated in this case.

Tests were run using the displacement triggering method with a 0.75kg and a 1kg trolley to determine if it was possible to use this algorithm for system identification (the figures show the results from the experiments using the 0.75kg trolley). The resulting gains were then used to calculate the system parameters. The ratio of the a_{21} parameters (which corresponds to k/m, was identified. As k remains constant, this ratio should be the same as the ratio of the two masses (which was 0.75 for this experimental setup). The results are shown in Figure 13, where a dotted line denotes the theoretical value of 0.75. It can be seen that the correlation between the experimental results and theoretical predictions is qualitatively good, in the presence of significant fluctuations above and below the theoretical value. The ratio of the
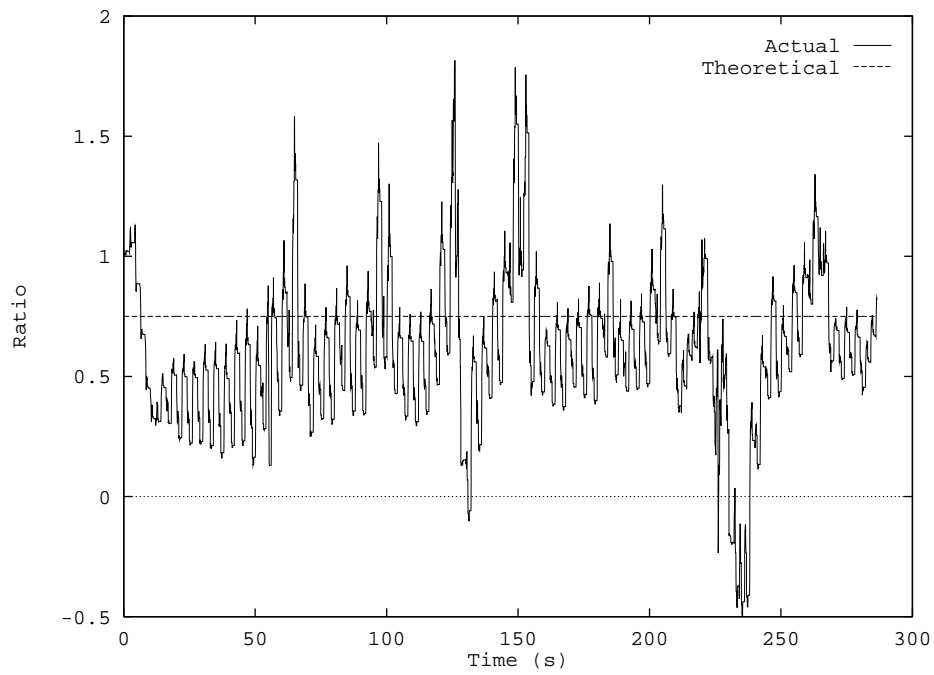
18

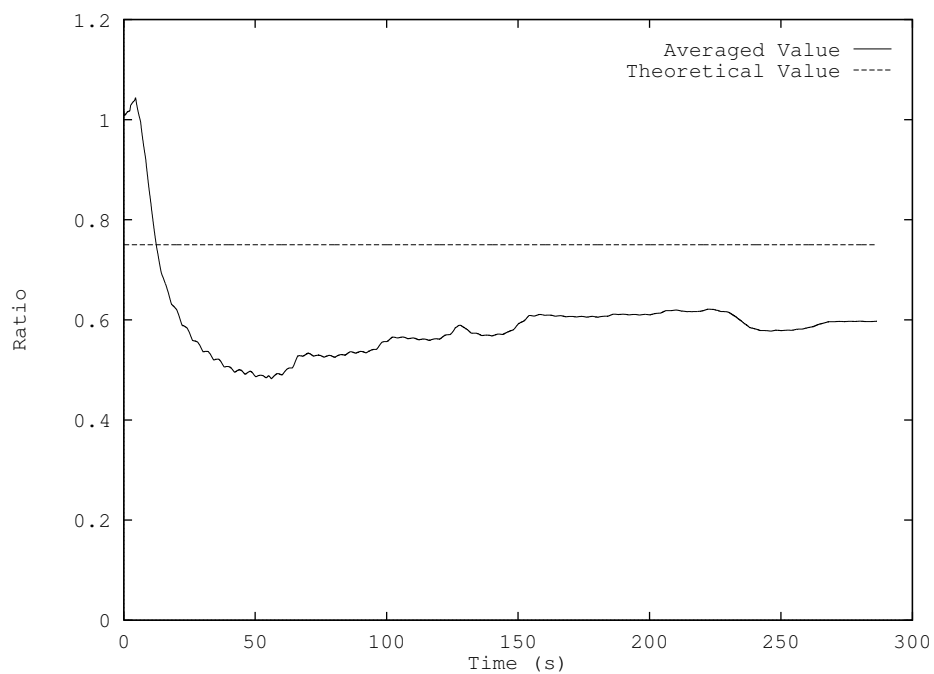Figure 13: Ratio of $a_{2,1}$ Parameters

Figure 14: Cumulative Average of Ratio of $a_{2,1}$ Parameters

a_{21} was recorded and averaged over a 78s period after the gains had stabilized and was found to be 0.6846. It was noted that the mean experimentally observed values for the system parameters tended to be lower than the predicted ones. The presence of large fluctuations is unavoidable, as we see from the adaptive gain plot in Figure 13. But taking a cumulative average over a period of time, Figure 14, shows the ratio converging to a steady value. Taking the averaged value across a suitably large steady state time range, we obtain estimated parameter values which are reasonably close to those predicted by theoretical calculations. This has been achieved using a modified linear adaptive algorithm in the presence of a strong impact nonlinearity which occurs at least once every forcing cycle.

5   Conclusions

In this paper a single degree of freedom spring-mass-damper experimental system was studied, which was subject to motion limiting constraints which led to impacts. The focus of this paper has been to determine if it is possible to carry out system identification of the system parameters, using adaptive control, in the presence of impacts. The unmodified adaptive control algorithm was found to destabilize via gain wind up in the presence of impacts. Three modified methods were investigated to try and improve this situation.

The first modified method used gain resetting after each impact. This stabilized the system, but did not allow system identification to be carried out. The second modified method used gain pausing at each impact. The gain wind up was still present and prevented system identification from being performed. The final modified method — based on displacement triggering — proved successful in both stabilizing the vibro-impact system, and in giving a estimation of the chosen system parameter with at least 80% accuracy.

Acknowledgments

References

Anderson, B. D. O., Bitmead, R. R., Johnson Jr, C. R., Kokotovic, P. V., Kosut, R. L., Mareels, I. M. Y., Praly, L. & Riedle, B. D. (1986). *Stability of adaptive systems: Passivity and averaging analysis.* MIT press: Cambridge Massachusetts.

Annaswamy, A.M. & Wong, J. (1997). Adaptive Control in the Presence of Saturation Non Linearity. *International Journal of Adaptive Control and Signal Processing* **11**, 3–19.

Bishop, S. R., Wagg, D. J. & Xu, D. (1998). Use of control to maintain period-1 motions during wind-up or wind-down operations of an impacting driven beam. *Chaos, Solitons and Fractals* **9**(1/2), 261–269.

Hodgson, S. P. & Stoten, D. P. (1996). Passivity-based analysis of the minimal control synthesis algorithm. *International Journal of Control* **63**(1), 67–84.

Hodgson, S. P. & Stoten, D. P. (1999). Robustness of the minimal control synthesis algorithm to non-linear plant with regard to the position control of manipulators. Preprint.

Ioannou, P. A. & Kokotovic, P. V. (1984). Instability analysis and improvement of robustness of adaptive control. *Automatica* **20**(5), 583–594.

Karagiannis, K. & Pfeiffer, F. (1991). Theoretical and experimental investigations of gear rattling. *Nonlinear dynamics* **2**, 367–387.

Kárason, S.P. & Annaswamy, A.M. (1994). Adaptive Control in the Presence of Input Constraints. *IEEE Transactions on Automatic Control* **39**(11), 2325–2330.

Knudsen, C., Feldberg, R. & True, H. (1992). Bifurcations and chaos in a model of a rolling railway wheelset. *Philosophical Transactions of the Royal Society of London A* **338**, 455–469.

McCarragher, B.J. & Austin, D.J. (1998). Model Adaptive Hybrid Dynamic Control for Constrained Motion Systems. *IEEE Transactions on Automatic*

Proc. IMechE. Part I: Journal of Systems & Control Engineering, 219: 121–132

    Control **43**(4), 560–564.

Neilson, R. D. & Gonsalves, D. H. (1993). Chaotic motion of a rotor system with a bearing clearance. In *Applications of fractals and chaos*, A. J. Crilly, R. A. Earnshaw, & H. Jones (Eds.), 285–303. Springer-Verlag.

Perterka, F. & Kotera, T. (1995). Different ways from chaotic motion in mechanical vibro-impact systems. In *Ninth World Congress on the Theory of Machines and Mechanisms*, Volume 2, Politecnico of Milano, Itay.

Sastry, S. & Bodson, M. (1989). *Adaptive control:Stability, convergence and robustness*. Prentice-Hall:New Jersey.

Sauer, T. (1994). Reconstruction of dynamical systems from interspike intervals. *Physical Review Letters* **72**(24), 3811–3814.

Stoten, D. P. (1993). An overview of the minimal control synthesis algorithm. In *I. Mech. E. Conference on Aerospace Hydraulics and Systems*, London. Paper C474-033.

Stoten, D. P. & Benchoubane, H. (1990). Robustness of a minimal controller synthesis algorithm. *International Journal of Control* **51**(4), 851–861.

Stoten, D. P. & Benchoubane, H. (1993). The Minimal Control Synthesis Identification Algorithm. *International Journal of Control* **58**(3), 685–696.

Theodossiades, S. & Natsiavas, S. (2001). Periodic and chaotic dynamics of motor-driven gear-pair system with backlash. *Chaos, Solitions and Fractals* **12**, 2427–2440.

Tung, P-C., Wang, S-R. & Hong, F-Y. (2000). Application of MRAC theory for adaptive control of a constrained robot manipulator. *International Journal of Machine Tools & Manufacture* **40**, 2083–2097.

Wagg, D. J., Karpodinis, G. & Bishop, S. R. (1999). An experimental study of the impulse response of a vibro-impacting cantilever beam. *Journal of Sound and Vibration* **228**(2), 243–264.

Zavala-Rio, A. & Brogliato, B. (2001). Direct adaptive control design for

one-degree-of-freedom complementary slackness jugglers. *Automatica* **37**, 1117–1123.